

# Inhomogeneous Big Bang Nucleosynthesis: Upper Limit on $\Omega_b$ and Production of Lithium, Beryllium, and Boron

Karsten Jedamzik\* and Jan B. Rehm†

*Max-Planck-Institut für Astrophysik, Karl-Schwarzschild-Str. 1, 85748 Garching, Germany*

(November 5, 2018)

We examine the Big Bang nucleosynthesis (BBN) process in the presence of small-scale baryon inhomogeneities. Primordial abundance yields for D,  $^4\text{He}$ ,  $^6\text{Li}$ ,  $^7\text{Li}$ ,  $^9\text{Be}$ , and  $^{11}\text{B}$  are computed for wide ranges of parameters characterizing the inhomogeneities taking account of all relevant diffusive and hydrodynamic processes. These calculations may be of interest due to (a) recent observations of the anisotropies in the cosmic microwave background radiation favoring slightly larger baryonic contribution to the critical density,  $\Omega_b$ , than allowed by a standard BBN scenario and (b) new observational determinations of  $^6\text{Li}$  and  $^9\text{Be}$  in metal-poor halo stars. We find considerable parameter space in which production of D and  $^4\text{He}$  is in agreement with observational constraints even for  $\Omega_b h^2$  a factor 2-3 larger than the  $\Omega_b$  inferred from standard BBN. Nevertheless, in this parameter space synthesis of  $^7\text{Li}$  in excess of the inferred  $^7\text{Li}$  abundance on the Spite plateau results. Production of  $^6\text{Li}$ ,  $^9\text{Be}$ , and  $^{11}\text{B}$  in inhomogeneous BBN scenarios is still typically well below the abundance of these isotopes observed in the most metal-poor stars to date thus neither confirming nor rejecting inhomogeneous BBN. In an appendix we summarize results of a reevaluation of baryon diffusion constants entering inhomogeneous BBN calculations.

## I. INTRODUCTION

The possibility that cosmic baryon number fluctuations may have existed on small scales in the early universe has received considerable attention between the late eighties and mid nineties [1–5]. Such fluctuations in baryon number would have impact on the production of light elements during BBN provided the baryonic mass of individual lumps exceeds  $M_b \gtrsim 10^{-21} M_\odot$ . It was speculated that production of inhomogeneities could result during a first-order QCD phase transition or even possibly during a scenario of electroweak baryogenesis. Initially it was hoped for that such scenarios could make BBN consistent with  $\Omega_b = 1$  and therefore eliminate the need for “exotic” non-baryonic dark matter. Detailed calculations revealed that inhomogeneous BBN (hereafter, IBBN) scenarios may not be consistent with a universe closed in baryons due to considerable overproduction of  $^7\text{Li}$  and/or  $^4\text{He}$ . At present,  $\Omega_b = 1$  seems also hardly desirable because of a variety of other arguments, such as the cosmological baryon budget [6], and the success of a structure formation scenario employing cold dark matter, among others.

Recently, observations of the cosmic microwave background radiation (hereafter; CMBR) on intermediate angular scales by the BOOMERANG and MAXIMA balloon missions have achieved unprecedented accuracy [7]. These missions have allowed for a first stab at an estimate of a number of cosmological parameters such as the total cosmic density parameter  $\Omega_{tot}$  and  $\Omega_b$ , among others. Common to both studies is the observation of a relatively suppressed CMBR power spectrum on scales where a secondary peak in the spectrum is anticipated compared to the power at the location of the first peak. Though preliminary, the conclusion of a number of au-

thors is that, within the parameters commonly allowed to be varied, an increased  $\Omega_b$  could most easily account for such a suppression [8]. (for alternative explanations cf. to Ref. [9]). This has lead to the preliminary claim that  $\Omega_b$  as inferred from CMBR anisotropy observations may be in conflict with the best estimate  $\Omega_b h^2 \approx 0.02 \pm 0.002$  from SBBN [10–12], in particular, the CMBR data would prefer  $\Omega_b h^2 \approx 0.03$  [8] ( $h$  is the Hubble constant in units of  $100 \text{ km s}^{-1} \text{ Mpc}^{-1}$ ). Note that even though, at first glance the deviation between these two values seems relatively small, it is clear that a baryonic density parameter of  $\Omega_b \approx 0.03 h^{-2}$  can not be achieved within a SBBN scenario. For such large  $\Omega_b$ , SBBN production of deuterium can neither account for the deuterium as observed in quasar absorption systems [13,11], nor for the inferred D abundance in the presolar nebula and only barely for the D as observed in the local interstellar medium.

Newly developed high-resolution spectrographs (such as UVES on the VLT) allow for a significant increase in the number of stars with claimed detections for the elements  $^6\text{Li}$  and  $^9\text{Be}$ . Whereas for a long time there had been only two claimed  $^6\text{Li}/^7\text{Li}$  [14] detections in low-metallicity PopII halo stars, this number is/will rapidly increase in the immediate future. Moreover,  $^6\text{Li}/^7\text{Li}$  detections have now also been claimed for disk stars at relatively high metallicities [15]. The preliminary picture which emerges is that  $^6\text{Li}/\text{H}$  abundances in stars are remarkably similar over a wide range in metallicities, though interpretation of the data has to account for the possibility of stellar  $^6\text{Li}$  astration. Recently, there has been an interesting  $^9\text{Be}/\text{H}$  detection within the atmosphere of a very low-metallicity star [16]. The  $^9\text{Be}/\text{H}$  abundance in this star is higher than expected from extrapolation of the approximately linear  $^9\text{Be}/\text{H}$  versus  $[\text{Fe}/\text{H}]$  relation such that this observation may represent

tentative evidence for a flattening of the  ${}^9\text{Be}/\text{H}$  versus  $[\text{Fe}/\text{H}]$  slope at metallicities below  $[\text{Fe}/\text{H}] < -3$ .

In light of the above, it seems worth reinvestigating BBN with an inhomogeneous baryon distribution. Whereas production of  ${}^6\text{Li}$  and  ${}^9\text{Be}$  in standard BBN is essentially negligible, it is known that production of these isotopes in IBBN may be significantly enhanced [17]. Furthermore, it should be of interest not only to find out of how much the upper limit on  $\Omega_b$  in IBBN may be relaxed compared to that from standard BBN, but also in how much of the parameter space, characterizing the inhomogeneities, IBBN abundance yields may agree with observational constraints.

## II. INHOMOGENEOUS BIG BANG NUCLEOSYNTHESIS CALCULATIONS

We have performed detailed numerical computations of IBBN by employing the IBBN code described in Ref [3]. This code treats all the relevant baryon diffusion of neutrons, protons, and lighter nuclei. In the Appendix we summarize the employed baryon diffusion constants for protons and neutrons, which includes a reevaluation of some diffusion constants and a correction for mistakes in the literature. The employed code is still the only existing code with a detailed treatment of the effects of photon diffusion and hydrodynamic expansion on the evolution of high-density regions [18,19]. It is known that these dissipative processes operating at lower temperatures  $T \lesssim 30\text{ keV}$  may affect the predicted abundances of  ${}^6\text{Li}$ ,  ${}^7\text{Li}$ ,  ${}^9\text{Be}$ , and  ${}^{11}\text{B}$  in some part of the parameter space (in particular, for compact high-density regions). For example,  ${}^7\text{Li}$  produced in form of  ${}^7\text{Be}$  may be prematurely destroyed by the reaction sequence  ${}^7\text{Be}(n,p){}^7\text{Li}$  ( $p,\alpha$ ) $\alpha$  when enough neutrons may be delivered to the high-density regions where most of the  ${}^7\text{Be}$  is produced. The magnitude of this process depends on the efficiency of hydrodynamic expansion which increases the surface area of high-density regions but also on the correct neutron- and proton- diffusion constants at low temperatures. Note that the distribution (and diffusion) of protons affects the diffusion of neutrons through neutron-proton nuclear scattering [28].

We have updated the nuclear reaction rates employed in the IBBN code from those based on the compilation by Caughlan & Fowler, as described in Smith *et al.* [20], to include the improved charged nuclei induced reactions as compiled by the NACRE collaboration [21]. Note that the modifications in predicted abundances, when the central values of the improved nuclear reaction rates of the NACRE compilation are employed, are fairly small for  ${}^2\text{H}$  and  ${}^4\text{He}$  but can be in the  $\sim 20\%$  -  $30\%$  range for  ${}^7\text{Li}$ ,  ${}^6\text{Li}$ ,  ${}^9\text{Be}$ , and  ${}^{11}\text{B}$  (cf. to Ref. [22]). Additional uncertainties in the computed abundances arise from appreciable error bars quoted in the NACRE compilations for a few reactions, such as  $\text{D}(p,\gamma){}^3\text{He}$ ,  ${}^3\text{He}(\alpha,\gamma){}^7\text{Be}$ , and

$\text{D}(\alpha,\gamma){}^6\text{Li}$ . In the context of SBBN, these additional uncertainties are of similar magnitude to those quoted above, with the exception of the  ${}^6\text{Li}$  abundance which is subject to very large uncertainties of  $\sim$  factor 3-4 in either direction [23,22]. Though it is beyond the scope of the present work to present a detailed systematic analysis of uncertainties in the prediction of abundances in IBBN scenarios due to reaction rate uncertainties, we will comment below if such uncertainties could impact our main conclusions. Note that all  ${}^4\text{He}$  mass fractions  $Y_p$  presented below are corrected by  $\Delta Y_p = +0.0049$  to account for a variety of physical effects as detailed in Ref. [24].

From the multitude of conceivable initial conditions for the baryon inhomogeneities (including stochastic ones as treated in Ref. [25]) we chose a regular lattice of spherical symmetric domains, approximating the possible outcome of baryon fluctuations generated during a first-order (e.g. QCD) phase transition around the shrinking bubbles of high-temperature phase. The spherical computation domain is then characterized by its physical length,  $l_{100}$ , specified at temperature of  $T = 100\text{ MeV}$  (specifically,  $1\text{ m}$  at  $T = 100\text{ MeV}$  is to be understood as a length of  $5.96 \times 10^{11}\text{ m}$  at the present epoch [26]). Within this domain we assume a region of high baryon density with baryon-to-photon ratio  $\eta_h$  occupying volume fraction  $f_V$  and a low density region at  $\eta_l = \eta_h/R$  occupying the remainder of the volume, with an initial discontinuity at the boundary of both regions (which softens after some baryon diffusion). This yields an average baryon-to-photon ratio

$$\eta = f_V R \eta_l + (1 - f_V) \eta_l. \quad (1)$$

Given these initial conditions there exist still four parameters to be specified, namely  $\eta$ ,  $l_{100}$ ,  $f_V$ , and  $R$ . The initial parameter space is reduced by assuming  $f_V R = 200$ . Physically  $f_V R \gg 1$  corresponds to essentially all baryons residing in the high-density region and none in the low-density region, such that for  $f_V R \gtrsim 10$  one obtains results essentially independent of the exact value of this parameter combination. Though the opposite limit,  $f_V R \ll 1$ , may be interesting for the production of significant amounts of isotopes with nucleon number  $A \geq 12$  [27], in much of the parameter space it yields only minor changes in the D,  ${}^4\text{He}$ , and  ${}^7\text{Li}$  as compared to a SBBN scenario at the same  $\eta$ . Our calculations employ two different initial “geometries”: (a) spherical condensed - where the high-density region resides at the center of the spherical domain and (b) spherical shell - where the high-density region occupies a shell at the outer edge of the computational domain. These spherical domains are finite-differenced into 24 zones. By increasing the number of zones we estimate that the relative error in predicted abundances does not exceed  $\sim 0.5\%$  for  ${}^4\text{He}$ ,  $\sim 3\%$  for D, and  $\sim 10\%$  for the shown isotopes with  $A \geq 7$ .

### III. RESULTS AND DISCUSSION

Figures 1 - 4 show computed abundance yields in IBBN scenarios for the isotopes of D,  $^4\text{He}$ ,  $^7\text{Li}$ , as well as  $^6\text{Li}$ ,  $^9\text{Be}$ , and  $^{11}\text{B}$  as a function of the length scale of the domains (approximately corresponding to the mean separation between fluctuations) for differing  $\Omega_b$  and a wide range of parameters describing the baryon inhomogeneities. The choice of the parameter space for which abundance yields are shown is supposed to bracket most potentially interesting  $\Omega_b$  (taking values of  $\Omega_b h^2 = 0.012, 0.025, 0.038$  and  $0.051$  shown by the solid, dotted, short-dashed, and long-dashed lines in each figure, respectively), as well as to illustrate the general trends of changing “geometry” (Figures 1 and 2 are for spherical condensed fluctuations, whereas Figure 3 and 4 are for spherical shells) and changing volume fractions  $f_V$  of the high-density regions. We have deliberately not indicated observationally inferred limits on the primordial abundances in these figures, as these are likely to change over the course of time, and since we are more interested in a qualitative understanding of IBBN abundance yields and their potential agreement/disagreement with observationally inferred abundance limits.

It is well known that there exists an “optimum” length scale where the  $^4\text{He}$  yield may be lower than in a SBBN scenario at the same  $\Omega_b$  due to the fact that neutrons may diffuse out of the high-density regions, subsequently decaying in the low-density region before they may be incorporated into  $^4\text{He}$ . This effect is more pronounced when  $f_V$  is small (Figures 1 and 3) since back-diffusion of neutrons into the high-density regions is less efficient. Similarly, one finds an “optimum”  $l_{100}$  where  $^7\text{Li}$  production is minimized, generally somewhat smaller than the length scale for minimum  $^4\text{He}$  production. Nevertheless, even at this “optimum” distance the  $^7\text{Li}$  yields are often higher, at best somewhat lower, than the  $^7\text{Li}$  yields in a SBBN scenario at the same  $\Omega_b$  and they increase with decreasing  $f_V$  [28]. These trends are due to the two different production mechanisms for  $^7\text{Li}$  (direct production in the low-density region and production of  $^7\text{Be}$  in the high-density region) and the relative efficiency of these mechanisms at either lower or higher  $\eta$  than the approximate  $\eta$  inferred from SBBN.

There are currently two mutually inconsistent observationally inferred values for the  $^4\text{He}$  mass fraction, i.e. a high value  $Y_p \approx 0.244$  [29] and a low value  $Y_p \approx 0.234$  [30,31]. It also becomes more and more appreciated that the inference of  $Y_p$  from observations of HII regions is subject to systematic errors of possibly considerable magnitude. Much progress has been made in the determination of primordial D abundances in quasar absorption line systems (QASs). There are now several QASs seemingly indicating low D/H  $\approx 2.5 - 4 \times 10^{-5}$  [13,11] and only one which favors high D/H  $\approx 2 \times 10^{-4}$  [32]. In light of this, one should probably demand from a successful BBN scenario to have  $Y_p < 0.25$  (conservative) and low D/H

$\approx 2 - 5 \times 10^{-5}$ . (Note that even within the context of a SBBN scenario, a D/H  $\approx 3 \times 10^{-5}$  abundance implies seemingly uncomfortably high  $Y_p \approx 0.247$  [10,11]. The figures illustrate that one may find considerable IBBN parameter space where these requirements on the primordial  $^4\text{He}$  and D/H abundances may be met, even for  $\Omega_b h^2$  as large as  $\sim 0.05$ . This is due to IBBN scenarios often yielding less  $^4\text{He}$  and more D production than a SBBN scenario at the same  $\Omega_b$ .

Nevertheless, these considerations disregard observational limits on the  $^7\text{Li}/\text{H}$  abundance. Typical  $^7\text{Li}$  yields in the IBBN parameter space which agree with observational limits on  $Y_p$  and D/H strongly depend on  $\Omega_b$  (as well as on geometry and  $f_V$ ), ranging between about  $3 \times 10^{-10}$  and  $10^{-8}$  for  $\Omega_b h^2 = 0.025$  and  $3 \times 10^{-9}$  to  $3 \times 10^{-8}$  for  $\Omega_b h^2 = 0.051$ . This is typically well in excess of the claimed primordial  $^7\text{Li}/\text{H} \approx 1.7 \times 10^{-10}$  as derived from observations of lithium abundances in metal-poor halo stars belonging to the Spite plateau. Though  $^7\text{Li}$  may in principle be depleted in these stars, there are strong arguments against this possibility, such as the claimed absence of intrinsic dispersion of  $^7\text{Li}$  abundances in stars belonging to the Spite plateau. Further, the more fragile  $^6\text{Li}$  isotope which should have been astrated as well, is by now observed in a few of these stars [34]. Recently, a primordial  $^7\text{Li}/\text{H}$  even as low as  $1.2 \times 10^{-10}$  has been claimed [35], which results from correcting  $^7\text{Li}$  abundances for galactic cosmic ray production of this isotope. Nevertheless, even an SBBN scenario (at  $\Omega_b h^2 = 0.02$ ) yields  $^7\text{Li}/\text{H} \approx 3.8 \times 10^{-10}$ , in excess of the primordial  $^7\text{Li}/\text{H}$  determination, when one assumes D/H  $3 \times 10^{-5}$  as favored by the QAS data. One thus would have to resort to a small amount of  $^7\text{Li}$  depletion and/or systematic errors due to, for example, the use of inappropriate stellar atmospheric models, to reconcile these values. If one demands the IBBN yield of  $^7\text{Li}$  to be at, or below, the quoted SBBN reference value, one finds that the  $\Omega_b h^2$  should be below 0.025, precluding a substantial increase of  $\Omega_b$  over that inferred from SBBN. Only if one were to relax the  $^7\text{Li}/\text{H}$  limit to about (seemingly unreasonable)  $10^{-9}$  could  $\Omega_b h^2$  in IBBN scenarios be consistent with the currently preferred  $\Omega_b h^2$  from CMBR anisotropy measurements  $\sim 0.03$ .

We have tested if these conclusions could be changed due to existing reaction rate uncertainties quoted by the NACRE collaboration [21]. We have changed the following reactions to their quoted limits: D(p, $\gamma$ ) $^3\text{He}$  (lower limit),  $^3\text{H}(\alpha, \gamma)^7\text{Li}$  (lower limit),  $^3\text{He}(\alpha, \gamma)^7\text{Be}$  (lower limit),  $^7\text{Li}(p, \alpha)^4\text{He}$  (upper limit), and D( $\alpha, \gamma$ ) $^6\text{Li}$  (upper limit). These changes have been “designed” to minimize  $^7\text{Li}$  production and maximize  $^6\text{Li}$  production. With these modified rates we have performed two calculations (a) spherical shell,  $\Omega_b h^2 = 0.038$ ,  $f_V^{1/3} = 0.025$ ,  $l_{100} = 724$  m, and (b) spherical condensed,  $\Omega_b h^2 = 0.038$ ,  $f_V^{1/3} = 0.0125$ ,  $l_{100} = 32$  m, where the length scales have been chosen close to the “optimum” distance for minimum  $^7\text{Li}$  production. This has led to a  $^7\text{Li}/\text{H}$  yield of

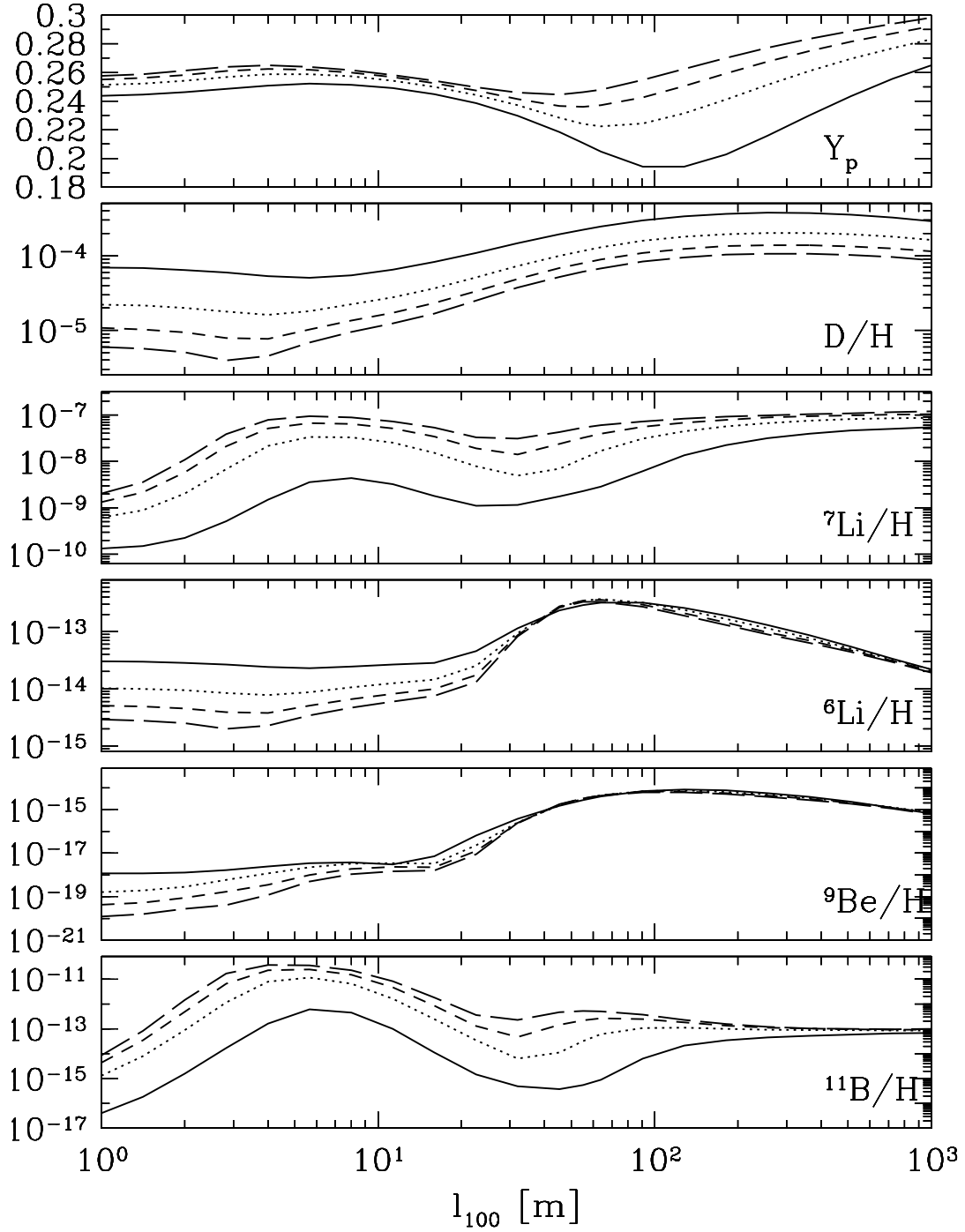


FIG. 1. Abundance yields of D,  ${}^4\text{He}$ ,  ${}^6\text{Li}$ ,  ${}^7\text{Li}$ ,  ${}^9\text{Be}$ , and  ${}^{11}\text{B}$  in IBBN scenarios as a function of the inhomogeneity length scale  $l_{100}$  (given in meters at  $T = 100$  MeV). The calculation assumes spherical condensed inhomogeneities with high-density volume filling fraction  $f_V = 0.125^3$  and density contrast between high- and low-density regions of  $R = 200/f_V$  (see text for details). Except for the  ${}^4\text{He}$  abundance which is given as mass fraction,  $Y_p$ , all abundances are given as number fractions relative to hydrogen as indicated in the panels. The solid, dotted, short-dashed, and long-dashed lines refer to results for  $\Omega_b h^2 = 0.012$ , 0.025, 0.038, and 0.051, respectively.

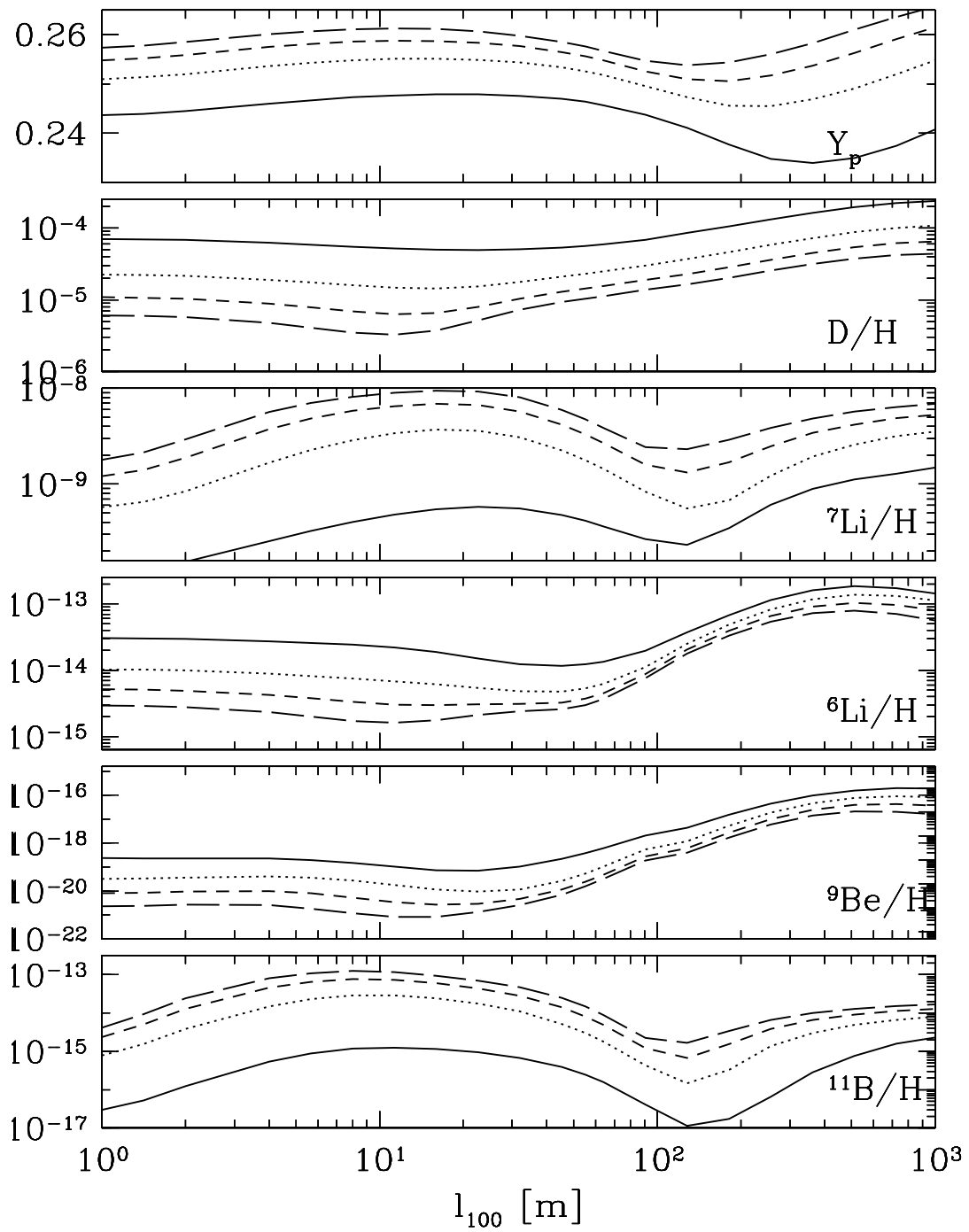


FIG. 2. As Figure 1, but for  $f_V = 0.5^3$ .

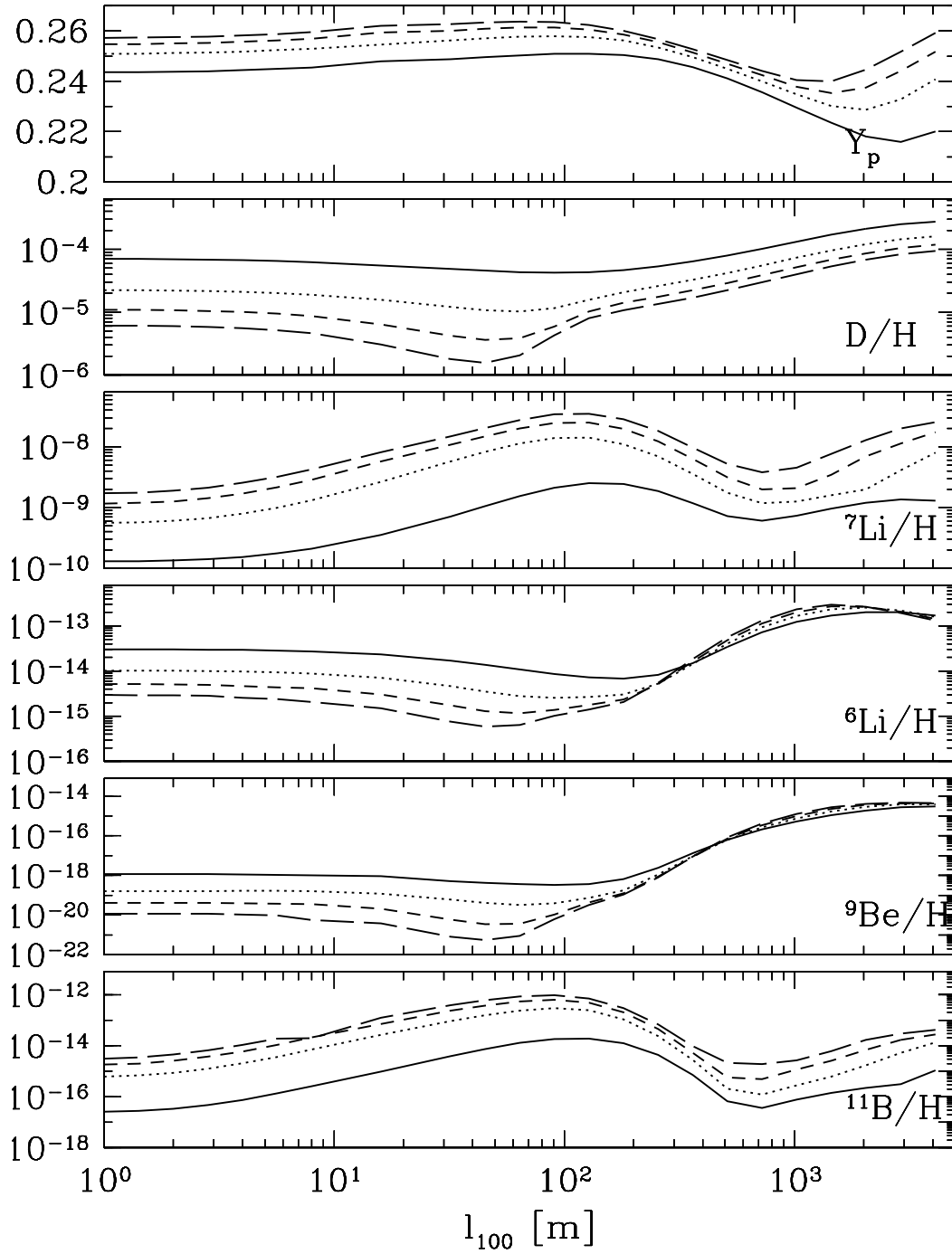


FIG. 3. As Figure 1, but for spherical shell geometry and  $f_\nu = 0.25^3$ .

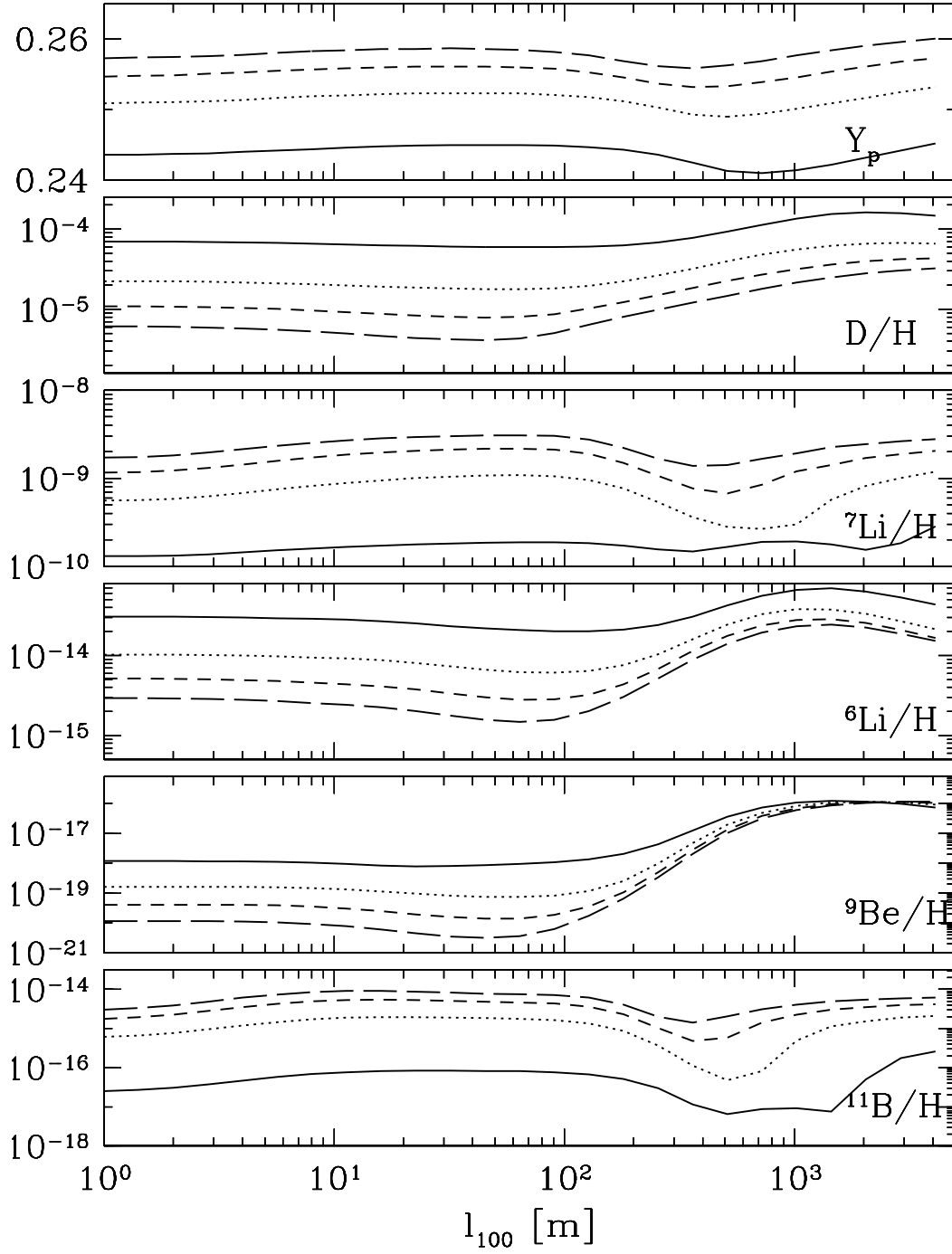


FIG. 4. As Figure 1, but for spherical shell geometry and  $f_V = 0.8^3$ .

$1.45 \times 10^{-9}$  (compared to  $2 \times 10^{-9}$  when the central values of the reaction rates are used) in case (a) and  $1.02 \times 10^{-8}$  (compared to  $1.4 \times 10^{-8}$ ) in case (b), illustrating that the uncertainty in the predicted  ${}^7\text{Li}$  remains within bounds. Nevertheless, a large uncertainty exists in the prediction for the  ${}^6\text{Li}$  abundance: we have found a factor  $\sim 3$  and 4 increase in case (a) and (b), respectively.

It should be interesting to explore if the abundance yields of  ${}^6\text{Li}$ ,  ${}^9\text{Be}$ , and  ${}^{11}\text{B}$  in IBBN scenarios may be as large as the abundances of these isotopes observed in the most metal-poor stars to date. Such a comparison could yield, in principle, independent confirmation/rejection of IBBN scenarios. In the parameter space where IBBN yields are consistent with observationally inferred limits on  ${}^4\text{He}$  and  $\text{D}/\text{H}$ , we find production of  ${}^6\text{Li}/\text{H} \sim 10^{-14} - 7 \times 10^{-13}$  (including the large reaction rate uncertainty in the  $\text{D}(\alpha, \gamma){}^6\text{Li}$  rate), implying a typical “maximum” enhancement factor for this isotope of about 10-30 compared to a SBBN scenario at the same  $\Omega_b$ . For the  ${}^9\text{Be}$  and  ${}^{11}\text{B}$  isotopes one finds ranges of  ${}^9\text{Be}/\text{H} \sim 10^{-18} - \text{a few} \times 10^{-15}$ , and  ${}^{11}\text{B}/\text{H} \sim 10^{-16} - 10^{-13}$ . Typical IBBN yields of these isotopes seem therefore still much below the observed  ${}^6\text{Li}/\text{H} \sim 7 \times 10^{-12}$  [14],  ${}^9\text{Be}/\text{H} \sim 5 \times 10^{-14}$  [36,16], and  ${}^{11}\text{B}/\text{H} \sim 10^{-12}$  [37] in the lowest metallicity stars to date where such observations have been performed. These observations are thus inconclusive with regards to a validation of IBBN scenarios. Though it is not easy to completely rule out the possibility that there indeed exist very specific initial conditions for the baryon inhomogeneities which yield primordial production of  ${}^6\text{Li}$ ,  ${}^9\text{Be}$ , and  ${}^{11}\text{B}$  in abundance as high as currently observed in the lowest metallicity stars, it seems clear that this is not the typical case.

In summary, we have performed numerical simulations of BBN in the presence of an inhomogeneous baryon distribution for wide ranges of the parameters describing the inhomogeneities and for a few representative baryon-to-photon ratios. Our choice of initial conditions is limited to scenarios where essentially all baryons are within overdense pockets and the remainder of the volume is initially void of baryons. We found that such scenarios may be consistent with observational limits on the primordial  ${}^4\text{He}$  and  $\text{D}$  abundance for  $\Omega_b h^2$  as large as  $\sim 0.05$ , however, they result in significantly overabundant production of  ${}^7\text{Li}$  with respect to the  ${}^7\text{Li}/\text{H}$  ratio as observed in stars belonging to the Spite plateau. We note here that similar conclusions have been recently drawn by Ref. [38]. Typical production of  ${}^6\text{Li}$ ,  ${}^9\text{Be}$ , and  ${}^{11}\text{B}$  in such scenarios are found to be still below the abundances of these isotopes observed in the most metal-poor stars to date. Unless  ${}^7\text{Li}$  in stars on the Spite plateau has been significantly overabundant, which seems unlikely, IBBN scenarios thus do not allow for a significant increase of  $\Omega_b$  over that inferred from a SBBN scenario.

We wish to acknowledge several useful discussions with In-Saeng Suh and Naoki Yoshida.

## APPENDIX A: REEVALUATION OF BARYON DIFFUSION CONSTANTS

In this appendix we summarize the baryon diffusion constants which we used in our inhomogeneous Big Bang nucleosynthesis calculations. Some of these diffusion constants have been reevaluated. Such a reevaluation seemed necessary not only since prior work on the subject [1,40] yielded partially conflicting results (e.g., the proton diffusion constant due to proton-electron scattering as computed by Applegate, Hogan, & Scherrer and Banerjee & Chitre), but also due to improvement on approximations, such as an energy independent neutron-proton cross section. Furthermore, we correct for the electron diffusion constant due to electron-photon scattering as given in [19]. Rather than going over the partially lengthy details of the calculations we performed, we will state our results, outline by what procedure we obtained them, and highlight the differences to prior evaluations.

Banerjee & Chitre [40] (hereafter; BC) computed diffusion constants by using the first-order Chapman-Enskog approximation for arbitrarily relativistic particles as thoroughly discussed in the monograph by de Groot, van Leeuwen, & van Weert [41] (hereafter; GLW). The master equation given in BC for the computation of diffusion constants (i.e., Eqs. (1), (3), and (4) in BC) are not directly evident from GLW but involve a fairly detailed computation. We have therefore redone the calculation of this master equation and arrive at the same result [39] as BC. Note that the first-order Chapman-Enskog approximation is typically accurate to within 20-30 % [41].

### (a) neutron-electron scattering

At higher temperatures ( $T \gtrsim 50 - 100$  keV), and when the local baryon-to-photon ratio ( $\eta$ ) is not too large, the diffusion of neutrons is limited by magnetic moment scattering off electrons and positrons. Using the master equations of BC, under the assumption of an energy-independent cross section, and to lowest non-trivial order in the small quantities  $m_e/m_N$  and  $T/m_N$ , where  $m_e$ ,  $m_N$ , and  $T$  are electron mass, nucleon mass, and temperature, respectively, but for arbitrary  $T/m_e$ , we find

$$D_{ne} = \frac{3}{8} \sqrt{\frac{\pi}{2}} \frac{1}{n_{e\pm} \sigma_{ne}^t} \frac{1}{z_e^{1/2}} \frac{K_2(z_e)}{K_{5/2}(z_e)}, \quad (\text{A1})$$

in agreement with BC. In this expression  $z_e = m_e/T$ , the quantity  $n_{e\pm}$  is the total number density of electrons and positrons, the transport cross section is

$$\sigma_{ne}^t = \int d\Omega \frac{d\sigma_{ne}}{d\Omega} (1 - \cos\theta), \quad (\text{A2})$$

to be evaluated in the center-of-mass system, and  $K_n$  are modified Bessel functions of the second kind and of  $n$ th order, i.e.

$$K_2(z) = \frac{1}{z^2} \int_0^\infty k^2 \exp(-\sqrt{k^2 + z^2}) dk, \quad (\text{A3})$$



and

$$K_{5/2}(z) = \sqrt{\frac{\pi}{2z}} e^{-z} \left( 1 + \frac{3}{z} + \frac{3}{z^2} \right). \quad (\text{A4})$$

The expression Eq. (A1) does agree with that derived by Applegate, Hogan, & Scherrer [1] (hereafter; AHS) via considering the drag force exerted by  $e^\pm$  on neutrons and using the Einstein relation. As noted by Ref. [42], both derivations of the diffusion constant approximate the fermionic occupation number by a relativistic Maxwellian, i.e.  $f = (\exp(E/T) + 1)^{-1} \approx \exp(-E/T)$ , which nevertheless should only result in a small error. Using  $\sigma_{ne}^t = 3\pi(\alpha\kappa/m_N)^2$ , with  $\alpha$  the fine structure constant and  $\kappa = -1.91$ , we may give a numerical value for the diffusion constant

$$D_{ne} = 1.87 \times 10^4 \frac{\text{m}^2}{\text{s}} \left( \frac{T}{\text{MeV}} \right)^{1/2} \frac{1}{(n_{e^\pm}/\text{MeV}^3)} \frac{K_2(z_e)}{K_{5/2}(z_e)}, \quad (\text{A5})$$

where  $n_{e^\pm}$  is given in natural units, i.e.  $\hbar = c = 1$ . The correct density  $n_{e^\pm}$  is easily obtained from the BBN code.

Recently Suh & Mathews [43,4] have considered finite-temperature effects on the neutron diffusion constant. They find a transport cross section due to neutron-electron (positron) magnetic moment scattering which significantly increases over  $\sigma_{ne}^t = 3\pi(\alpha\kappa/m_N)^2$  at low  $T \lesssim 0.5 \text{ MeV}$ . Since finite-temperature effects should vanish in the limit  $T \rightarrow 0$  their result is fairly surprising. We have therefore reevaluated the neutron-electron cross section by using the result given in Ref. [44] and confirm that neutron-electron scattering is independent of energy for electron energies much below the nucleon mass. Similarly, the authors claim a significant increase of  $D_{ne}$  at high  $T$  [4]. Within the context of their analysis, such an increase could only occur due to a change in the electron mass and/or the transport cross section. Nevertheless, according to their own analysis both quantities don't seem to deviate much from their zero-temperature limits for temperatures below  $T \lesssim 3 - 5 \text{ MeV}$ . In light of these inconsistencies we therefore prefer to use the standard AHS and BC results in our calculations.

### (b) neutron-proton scattering

Neutron-proton nuclear scattering limits diffusion of neutrons at lower temperatures and/or high  $\eta$ . At the low energies relevant for BBN the scattering cross section is dominated by scattering-angle independent s-wave scattering (zero angular momentum) resulting in a transport cross section which equals the total cross section,

$$\sigma_{np} = \frac{\pi a_s^2}{(a_s k)^2 + (1 - \frac{1}{2} r_s a_s k^2)^2} + \frac{3\pi a_t^2}{(a_t k)^2 + (1 - \frac{1}{2} r_t a_t k^2)^2}. \quad (\text{A6})$$

In this expression  $k$  is the nucleon wave vector in the center-of-mass (!) system [45], and the parameters

$a_s = -23.71 \text{ fm}$ ,  $a_t = 5.432 \text{ fm}$ ,  $r_s = 2.73 \text{ fm}$ , and  $r_t = 1.749 \text{ fm}$ . Only at very low temperatures the above cross section is approximately independent of energy. In that case, one may derive [41]

$$D_{np} = \frac{3\sqrt{\pi}}{8} \frac{1}{n_p \sigma_{np}} \left( \frac{T}{m_N} \right)^{1/2}, \quad (\text{A7})$$

for the diffusion constant, which is a factor of two smaller than the result given in BC. Nevertheless, the energy dependence of the cross section becomes large at  $T \gtrsim 50 \text{ keV}$  and should be taken into account. This may be done properly by evaluating the diffusion constant via the master equations in BC with the appropriate cross section Eq.(A6). Following this procedure we derived the cross section

$$D_{np} = 2.82 \times 10^{-5} \frac{\text{m}^2}{\text{s}} \left( \frac{T}{\text{MeV}} \right)^{1/2} \frac{1}{(n_p/\text{MeV}^3)} \times \frac{1}{I(a_1, b_1) + 0.16I(a_2, b_2)}, \quad (\text{A8})$$

where

$$I(a, b) = \frac{1}{2} \int_0^\infty dx \frac{x^2 e^{-x}}{ax + (1 - bx/2)^2}, \quad (\text{A9})$$

are integrals to be evaluated numerically. Here the parameters  $a$  and  $b$  are given by  $a_1 = 13.59 (T/\text{MeV})$ ,  $b_1 = -1.56 (T/\text{MeV})$ ,  $a_2 = 0.71 (T/\text{MeV})$ , and  $b_2 = 0.23 (T/\text{MeV})$ . We note that the integral  $I(a, b)$  converges only slowly against its limiting value  $I(0, 0) = 1$  as the temperature is decreased. In that limit, Eq. (A8) converges against Eq. (A7) with  $\sigma_{np} = \pi a_s^2 + 3\pi a_t^2$ .

### (c) proton-electron scattering

The diffusion of protons in IBBN scenarios is only significant at lower temperatures. As long as Debye screening of proton charge in the plasma is effective, protons may diffuse independently of the additional (net) electrons required by charge neutrality (cf. electron-photon scattering). In that case, proton diffusion is limited by Coulomb scattering on  $e^\pm$ . Both, AHS and BC compute the proton diffusion constant due to Coulomb scattering  $D_{pe}$ . However, their results differ by as much as a factor of eight at low temperatures. We have therefore recomputed  $D_{pe}$  by using the master equations given in BC and employing the Mott scattering cross section. To lowest order in  $m_e/m_N$ , and accurate to first order in  $T/m_e$ , we obtain

$$D_{pe} = \frac{3}{4\sqrt{2\pi}} \frac{T^2}{\alpha^2 n_{e^\pm}} \left( \frac{T}{m_e} \right)^{1/2} \frac{1 + \frac{15}{8} \frac{T}{m_e}}{\Lambda + 2 \frac{T}{m_e} (\Lambda - 1)}, \quad (\text{A10})$$

where  $\Lambda$  is the well-known Coulomb logarithm with  $\Lambda \approx \ln(T^2 m_e / 2\pi \alpha n_{e^\pm})^{1/2}$ . In the limit  $T/m_e \rightarrow 0$  Eq. (A10) reproduces the result of AHS. We conclude that  $D_{pe}$  as calculated by BC is a factor of eight to small at low  $T$ .

Deviations between Eq. (A10) and the result of AHS to first order in  $T/m_e$  are due to AHS approximating the electron energy in the Mott scattering cross section by  $m_e$ . Eq. (A10) yields for the numerical value of the proton diffusion constant

$$D_{pe} = 9.29 \times 10^{-2} \frac{\text{m}^2}{\text{s}} \left( \frac{T}{\text{MeV}} \right)^{5/2} \frac{1}{(n_{e\pm}/\text{MeV}^3)} \times \frac{1 + \frac{15}{8} \frac{1}{z_e}}{(\Lambda/5) + \frac{2}{z_e} ((\Lambda/5) - 1/5)}. \quad (\text{A11})$$

#### (d) electron-photon scattering

With the decrease of temperature thermally produced electron-positron pairs become rare and Debye screening of nuclear charge becomes inefficient. In this limit, electric forces which would rapidly be build up if the proton- and (net) electron- distributions differed, prevent the independent diffusion of these two species [19]. One may show, by evaluating the electric fields which would be present due to differing proton- and electron- distributions in the presence of Debye screening, and by comparison of the resulting proton flux due to the electric fields with the flux of protons due to diffusion, that protons may only diffuse independently, when  $n_{e\pm} \gg n_{e-} - n_{e+}$ . When this is not the case, electrons and protons diffuse together by ambipolar diffusion, with the effective diffusion constant given by twice that of the larger of electron- and proton- diffusion constants [46]. Electron diffusion is rendered fairly inefficient due to Thomson scattering of electrons on the cosmic background photons. The diffusion constant may be computed by considering the drag force on an electron due to a photon blackbody [47]

$$f_{\text{drag}} = \frac{4}{3} \frac{\pi^2}{15} \sigma_{\text{Th}} T^4 v, \quad (\text{A12})$$

with  $\sigma_{\text{Th}} \approx 6.65 \times 10^{-29} \text{m}^2$  the Thomson cross section and  $v$  the velocity of the electron in the cosmic background photon rest frame. Note that Eq. (A12) is given in natural units. Using Eq. (A12) together with the Einstein relation  $D = Tb$ , where the mobility  $b$  is defined as the proportionality constant between the terminal velocity  $v$  which a particle reaches in a plasma when an external force  $f$  is applied, i.e.  $v = bf$ , one finds for the effective proton diffusion constant

$$D_p^{\text{eff}} = 2D_e = 7.86 \times 10^{-2} \frac{\text{m}^2}{\text{s}} \left( \frac{T}{\text{MeV}} \right)^{-3}, \quad (\text{A13})$$

applicable when  $n_{e+} < n_{e-}$ . We note here that Eq. (A13) is different from the simple estimate given in Ref. [19]. We stress that the neglect of  $D_p^{\text{eff}}$  due to Thomson scattering, typically important at low  $T \lesssim 40 \text{keV}$ , may lead to errors in the calculated  ${}^7\text{Li}$  abundances by more than an order of magnitude.

- [1] J. H. Applegate, C. J. Hogan, & R. J. Scherrer, *Phys. Rev.* **D35**, 1151 (1987).
- [2] C. Alcock, G.M. Fuller, & G.J. Mathews, *Astrophys. J.* **320**, 439 (1987); R.M. Malaney & W.A. Fowler, *Astrophys. J.* **333**, 14 (1988); H. Kurki-Suonio, R. A. Matzner, J. M. Centrella, T. Rothman, & J. R. Wilson, *Phys. Rev.* **D38**, 1091 (1988); N. Terasawa & K. Sato, *Phys. Rev.* **D39**, 2893 (1989); G. J. Mathews, B. S. Meyer, C. R. Alcock, & G. M. Fuller, *Astrophys. J.* **358**, 36 (1990); G. J. Mathews, T. Kajino, & M. Orito, *Astrophys. J.* **456**, 98 (1996).
- [3] K. Jedamzik, G. M. Fuller, & G. J. Mathews, *Astrophys. J.* **423** 50 (1994).
- [4] In-Saeng Suh & G. J. Mathews, *Phys. Rev.* **D58**, 123002 (1998).
- [5] K. Kainulainen, H. Kurki-Suonio, & E. Sihvola, *Phys. Rev.* **D59**, 083505 (1999) and references therein.
- [6] M. Fukugita, C. J. Hogan, & P. J. E. Peebles, *Astrophys. J.* **503**, 518 (1998).
- [7] P. de Bernardis *et al.*, *Nature (London)* **404**, 955 (2000); S. Hanany *et al.*, *Astrophys. J. Letters* **545**, L5 (2000).
- [8] A. Balbi *et al.*, *Astrophys. J. Letters* **545**, L1 (2000); M. Tegmark and M. Zaldarriaga, *Phys. Rev. Lett.* **85**, 2240 (2000); J. Lesgourgues and M. Peloso, *Phys. Rev.* **D62** 081301 (2000); A. E. Lange *et al.*, *astro-ph/0005004*; W. Hu, M. Fukugita, M. Zaldarriaga, & M. Tegmark, *astro-ph/0006436*; A. H. Jaffe *et al.*, *astro-ph/0007333*; J. R. Bond *et al.*, *astro-ph/0011378*.
- [9] M. White, D. Scott, & Elena Pierpaoli, *Astrophys. J.* **545** 1 (2000); P. J. E. Peebles, S. Seager, & W. Hu, *Astrophys. J. Letters* **539**, L1 (2000); F. R. Bouchet, P. Peter, A. Riazuelo, & M. Sakellariadou, *astro-ph/0005022*.
- [10] S. Burles, K. M. Nollett, & M. S. Turner, *astro-ph/0008495*.
- [11] J. M. O'Meara, D. Tytler, D. Kirkman, N. Suzuki, J. X. Prochaska, A. M. Wolfe, *astro-ph/0011179*.
- [12] cf. also to K. A. Olive, G. Steigman, & T. P. Walker, *Phys. Rept.* **333**, 389 (2000).
- [13] S. Burles & D. Tytler, *Astrophys. J.* **499**, 699 (1998); *Astrophys. J.* **507**, 732 (1998); D. Tytler, J. M. O'Meara, N. Suzuki, & D. Lubin, *Physics Reports* **333**, 409 (2000).
- [14] V. V. Smith, D. L. Lambert, & P. E. Nissen, *Astrophys. J.* **408**, 262 (1993); L. M. Hobbs & J. A. Thorburn, *Astrophys. J.* **491**, 772 (1997); V. V. Smith, D. L. Lambert, & P. E. Nissen, *Astrophys. J.* **506**, 405 (1998), R. Cayrel, M. Spite, F. Spite, E. Vangioni-Flam, M. Cassé, & J. Audouze, *Astron. & Astrophys.* **343**, 923 (1999); P. E. Nissen, M. Asplund, V. Hill, & S. D'Odorico, *Astr. & Astrophys. Lett.* **357**, L49 (2000).
- [15] P. E. Nissen, D. L. Lambert, F. Primas, & V. V. Smith, *Astr. & Astrophys.* **348**, 211 (1999).
- [16] F. Primas, M. Asplund, P. E. Nissen, & V. Hill, *Astr. & Astrophys. Lett.* **364**, L42 (2000).
- [17] R. N. Boyd & T. Kajino, *Astrophys. J. Lett.* **336**, L55 (1989); R. A. Malaney & W. A. Fowler, *Astrophys. J. Lett.* **345**, L5 (1989); D. Thomas, D. N. Schramm, K. A. Olive, & B. D. Fields, *Astrophys. J.* **406**, 569 (1993); M. Orito, T. Kajino, R. N. Boyd, & G. J. Mathews, *Astrophys. J.* **488**, 515 (1997).
- [18] C. R. Alcock, D. S. Dearborn, G. M. Fuller, G. J. Math-

- ews, and B. S. Meyer, Phys. Rev. Lett. **64**, 2607 (1990).
- [19] K. Jedamzik & G. M. Fuller, Astrophys. J. **423**, 33 (1994).
- [20] M. S. Smith, L. H. Kawano, & R. A. Malaney, Astrophys. J. Suppl. **85**, 219 (1993).
- [21] C. Augulo *et al.* (The NACRE collaboration), Nucl. Phys. **A656**, 3 (1999) <http://pntpm.ulb.ac.be/nacre.htm>.
- [22] E. Vangioni-Flam, A. Coc, & M. Cassé, Astr. & Astrophys. **360**, 15 (2000).
- [23] K. M. Nollett, M. Lemoine, & D. N. Schramm, Phys. Rev. **C56**, 1144 (1997).
- [24] R. E. Lopez & M. S. Turner, Phys. Rev. **D59**, 103502 (1999).
- [25] H. Kurki-Suonio, K. Jedamzik, & G. J. Mathews, Astrophys. J. **479** 31 (1997).
- [26] Here we assumed a statistical weight of  $g_{\text{eff}} = 10.75$  at  $T = 100$  MeV and  $g_{\text{eff}} = 3.909$  at the present epoch, thus neglected muon and pion annihilation and assumed the completion of the cosmic quark-gluon transition.
- [27] K. Jedamzik, G. M. Fuller, G. J. Mathews, & T. Kajino, Astrophys. J. **422**, 423 (1994).
- [28] We have found that production of  ${}^7\text{Be}$  may be reduced by more than an order of magnitude if one (incorrectly) neglects the contribution of Thomson scattering to the proton diffusion constant (cf. Appendix). This may explain the discrepancies between our conclusions to be drawn below and the conclusions reached in Ref. [4].
- [29] Y. I. Izotov & T. X. Thuan, Astrophys. J. **500**, 188 (1998).
- [30] K. A. Olive, G. Steigman, & E. D. Skillman, Astrophys. J. **483**, 788 (1997).
- [31] M. Peimbert, A. Peimbert, & M. T. Ruiz, Astrophys. J. **541**, 688 (2000).
- [32] J. K. Webb *et al.*, Nature (London) **388**, 250 (1997).
- [33] P. Bonifacio & P. Molaro, Mon. Not. Roy. Astron. Soc. **285**, 847 (1997).
- [34] M. Lemoine, D. N. Schramm, J. W. Truran, & C. J. Copi, Astrophys. J. **478**, 554 (1997).
- [35] S. G. Ryan, T. C. Beers, K. A. Olive, B. D. Fields, & J. E. Norris, Astrophys. J. Lett. **530**, L57 (2000).
- [36] A. M. Boesgaard, C. P. Deliyannis, J. R. King, S. G. Ryan, S. S. Vogt, & T. C. Beers, Astron. J **117**, 1549 (1999).
- [37] R. J. Garcia Lopez, D. L. Lambert, B. Edvardson, G. Gustafsson, D. Kiselman, & R. Rebolo, Astrophys. J. **500**, 241 (1998).
- [38] H. Kurki-Suonio & E. Sihvola, astro-ph/0011544.
- [39] Note that in Eq.(4) of BC  $d\sigma_{ij}$  is the differential scattering cross section  $d\sigma_{ij}/d\Omega$  in the centre-of-mass system,  $\theta$  is the scattering angle in that reference system, and  $c M_{ij} t$ , the first argument in  $d\sigma_{ij}$  in Eq.(4) of BC, is to be associated with the total energy  $\sqrt{s}$  within the center-of-mass system. Furthermore, in comparing results between BC and GLW one needs to keep in mind that  $\sigma_{12}$  quoted in the diffusion constants given in GLW (computed under the assumption of energy- and angle- independent cross sections) is not the total cross section but that quantity divided by  $(4\pi)$ .
- [40] B. Banerjee & S. M. Chitre, Phys. Lett. **B258**, 247 (1991).
- [41] S. R. de Groot, W. A. van Leeuwen, & C. G. van Weert, *Relativistic Kinetic Theory* (North Holland, Amsterdam, 1980).
- [42] H. Kurki-Suonio, M. B. Aufderheide, F. Graziani, G. J. Mathews, B. Banerjee, & S. M. Chitre, Phys. Lett. **B289**, 211 (1992).
- [43] In-Saeng Suh & G. J. Mathews, Phys. Rev. **D58**, 025001 (1998).
- [44] H. M. Pilkuhn, *Relativistic Particle Physics* (Springer-Verlag, Heidelberg, 1979).
- [45] J. M. Blatt & V. F. Weisskopf, *Theoretical Nuclear Physics* (Springer-Verlag, New York, 1979).
- [46] L. D. Landau & E. M. Lifshitz, *Physical Kinetics* (Pergamon Press, Oxford, 1981).
- [47] P. J. E. Peebles, *Principles of Physical Cosmology* (Princeton Series in Physics 1993).